International Journal of Applied Power Engineering (IJAPE)
Vol.7, No.2, August 2018, pp. 166~180
ISSN: 2252-8792 DOI: 10.11591/ijape.v7.i2.pp166-180

Modelling and Control Design for Energy Management of Grid Connected Hybrid PV-wind System

Hassan Abouobaida, Said El Bied
Laboratory of Engineering Sciences for Energy (Labsipe), National School of Applied Sciences (ENSA) of El Jadida, University Research Center (URC), Chouaib-Doukkali University, Morocco

Article Info

Article history:

Received Mar 12, 2018
Revised May 20, 2018
Accepted May 31, 2018

Keywords:

Hybrid
MPPT
PV
TLBC
Wind

ABSTRACT

This paper deals with the control of hybrid PV-WIND power conversion structure. This paper develops a very important contribution which is the use of a single DC to DC converter, linearization of control of the Three-Level Boost Converter (TLBC) considering the imperfections of the passive components. The TLBC control provides balancing of capacitor voltages and maximum power operation of PV generator. For reasons of simplicity, a linearization based on the dynamic compensation of the disturbance is proposed. A sensorless Maximum Power Point Tracking (MPPT) algorithm is used to maximize a power extracted of the wind generator. The proportional relation between the rotational speed and the output voltage of the rectifier allows to use a voltage sensor to estimate the DC bus voltage reference instead of a mechanical speed sensor. The control of the three-phase inverter allows a transfer of the active power, the power factor close to the unit and thus a limitation of the reactive power injected into the grid. The external control loop performs the regulation of the common DC bus voltage while the internal control loop regulates the dq components of the currents injected into the grid. The simulation results showed the validity of the control approach. The proposed power conversion structure based on a single static converter has shown very good performance in terms of efficiency, the quality of the energy produced, complementarity between the two renewable sources and reliability. The paper ends with conclusions.

Corresponding Author:

Hassan Abouobaida,
Laboratory of Engineering Sciences for Energy (Labsipe),
National School of Applied Sciences (ENSA) of El Jadida, University Research Center (URC),
Chouaib-Doukkali University, Morocco.
Email: abouobaida.h@ucd.ac.ma

1. INTRODUCTION

In recent decades, the use of PV and wind resources has opened opportunities for the exploitation of renewable resources in the production of electric power. In wind generating systems that operate at variable speed and variable frequency, with the possibility of operating within a wider range of wind speed, and a significant reduction in mechanical stress provides better efficiency across the range of the wind speed. Even if the PV/wind sources are intermittent, the combination of these two sources is a good possibility to extract the maximum of the available natural energy since each source complement the other. The authors [1-2] show that the use of the hybrid PV/Wind source is considered an optimal solution because this source will remove the random aspect in case of a weak electrical network. Wang and Lin [3] proposes the study of a hybrid PV/wind system with the use of batteries. The system studied has allowed a significant improvement in reliability and flexibility. A PV/Wind autonomous hybrid system is discussed in [4]. The voltage is properly regulated at the load terminals, but the system is not reliable and cannot satisfy the energy requirement of the load. To overcome this problem, a hybrid system that includes PV/WIND/Fuel generator

is used in [5]. Giraud and Salameh [6] discusses a hybrid system connected to the grid with the use of storage batteries and which ensures a good system reliability.

Ensuring the continuity of power generation, designing the more reliable and low-cost power generation system, and producing higher quality power are usually the most common challenges in the design of power generation systems based on renewable sources.

The difficulty related to the exploitation of renewable sources is that these sources are intermittent, the electrical energy produced is not stable and strongly dependent on the climatic conditions. To overcome this problem, two or more renewable sources are inserted and exploited simulataneously in a production plant and therefore compliment each other. The other constraint is the design cost of the production plant. To minimize the cost of implementation, limiting the number of static converters is a better solution. In addition to miniaturization, this alternative is promising, it requires a low-cost control circuit (DSP or microcontroller card). This observation is justified by the minimization of the number of converters to be controlled (a single DC/DC converter instead of two DC/DC converters and a single DC/AC converter). Indeed, for the control of two static converters, less hardware and software resources are needed, so a less powerful control card, and a simple control program is sufficient (less complexity).

The present paper deals with the study of a grid connected hybrid PV/WIND system with a minimum number of converters. The studied structure allows the extraction and transfer of maximum PV/Wind power. Several works in the literature have discussed the combination of PV and WIND sources. A hybrid system based on PV, Wind and batteries are discussed in [7]. The studied system is characterized by a common DC bus and each source is linked to its own adaptation circuit. The common DC Bus is connected to the grid through an inverter. Bae and Kwasinski [8] presents a study of a hybrid system connected to the grid with the use of PV/PMSG sources. But the MPPT control is not implemented in this work. Several configurations are reported using PV/Wind in [9, 10]. The work [11] describes a PV/Wind hybrid system connected to a single-phase electrical grid. In this work, the author proposes a study where the PV generator is connected directly to the common DC bus. An uncontrolled three-phase rectifier followed by a DC/DC converter and a single-phase inverter are chosen. The extraction of maximum power of the PV generator is ensured by adjusting the DC bus voltage. The reference of the current injected into the grid is calculated from the variations of the DC bus current and the photovoltaic current. The control strategy ensures maximization and the transfer of the active power and the regulation of the DC bus voltage. The works of the literature have shown that each PV or PMSG sources in hybrid structures is associated to a power electronics converter. For better performance, each source (PV or wind) is controlled for maximum power operation. The control is realized by an algorithm called MPPT.

In this paper, a better efficiency is obtained by minimizing the number of DC/DC converters. The control approach has maximized the transfer of active power, regulation of the continuous common DC bus voltage and regulation of the speed of the wind generator. The MPPT method is used to extract the maximum power of the PV and PMSG generators. The use of the PWM control is currently more solicited in the control of the converters as adaptation circuits between AC and DC system, for obtaining a power factor close to unity. Other work in the literature deals with the study of hybrid PV/WIND systems based on a three-phase rectifier controlled. The three-phase rectifier makes it possible to raise the input voltage to a higher value of its created voltage. This type of converter is used between PMSG generator and the common DC bus [12-14]. In this work, a control strategy is proposed for a hybrid system PV/WIND subjected to very rapid changes of the wind speed and the solar irradiation. The proposed structure transfers the maximum power with better robustness regarding climate change. To minimize the number of DC/DC converters, the proposed structure includes a three-level boost converter and a three-phase inverter. The wind generator is directly connected to the common DC bus through a uncontrolled three-phase rectifier. Linear (PI) controllers ensure maximum power transfer, regulate the DC bus voltage and transfer the active power to the grid with a quasi-unit power coefficient. These functions are realized simultaneously making the hybrid PV/Wind system more more reliable and suitable for domestic and industrial applications.

2. HYBRID PV/WIND SYSTEM MODELING

The proposed hybrid power conversion system consists a three-phase uncontrolled diode rectifier, a TLBC and a three-phase inverter powered by photovoltic and wind source is shown in Figure 1 [15-16].

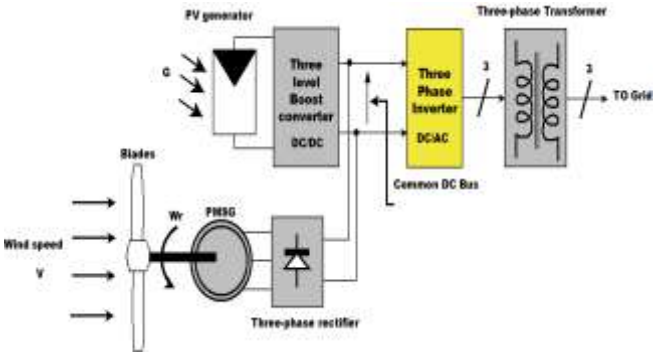

Figure 1. Proposed hybrid PV-wind power conversion system

The aim of this section is to give a mathematical model of the various power converters, the model of the PV and the PMSG generators as well as the mechanical part of the wind system. The model is based on the equations using steady-state equations and dynamic model of each part of the proposed hybrid system.

2.1. Photovoltaic system modeling

The photovoltaic conversion portion includes a PV generator and a TLBC as shown in Figure 2.

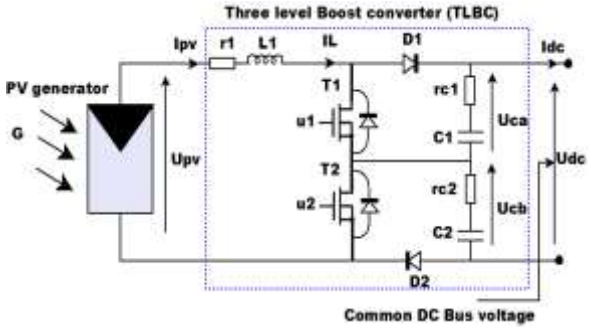

Figure 2. Power conversion system based a PV generator and the TLBC

2.1.1. PV model

The equivalent-circuit model and the power curve of the PV generator are illustrated in Figure 3 [17-18].

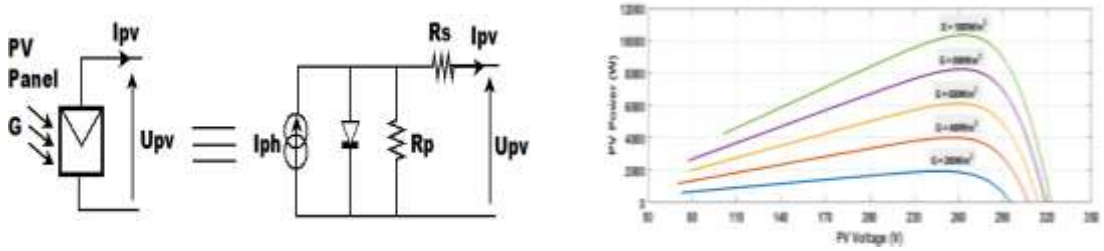

(a) (b)

Figure 3. (a) Equivalent model of the PV generator, (b) Power curve of the PV generator

2.1.2. TLBC model

The possibilities of the switching states of the power switches in TLBC are illustrated in Figure 4.

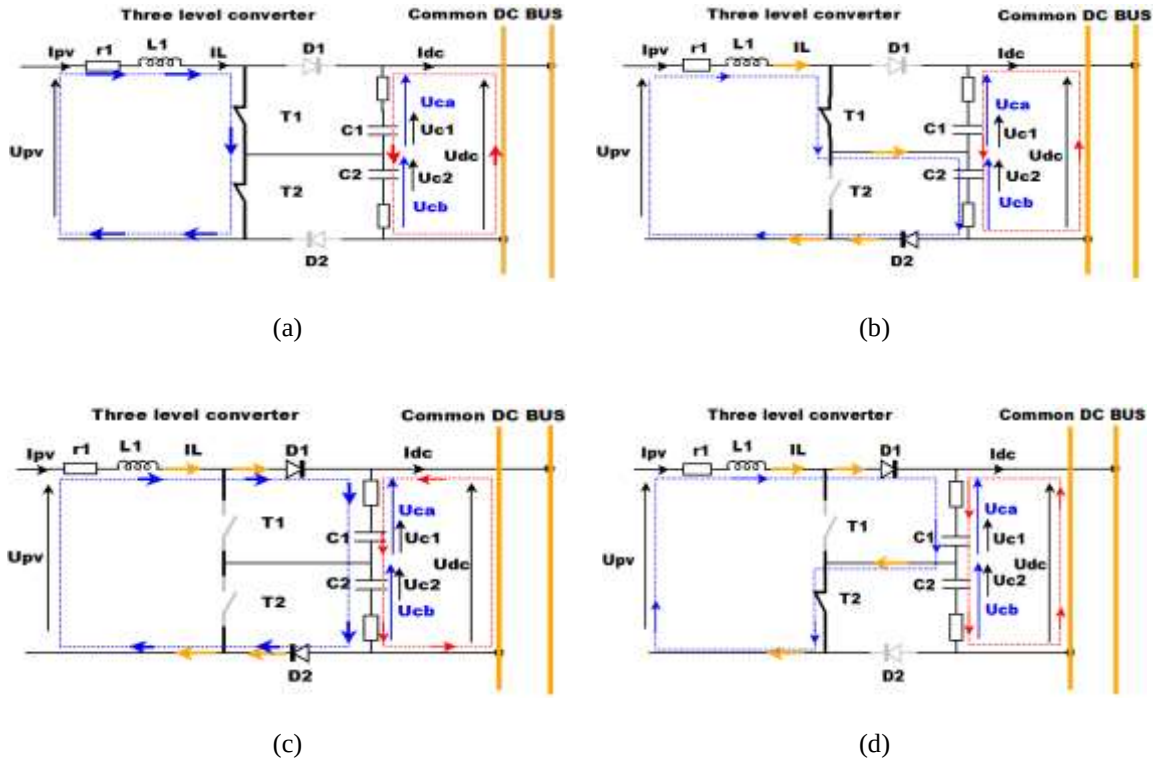

Figure 4. Possible switching states in (TLBC) Converter: (a) State 1; (b) State 2; (c) State 3; and (d) State 4

The dynamics model of TLBC is expressed by the following equations:

$$\dot{x} = A.x + B \tag{1}$$

By replacing x, A and B with their expressions, the dynamics of TLBC is expressed by the following matrix:

$$\begin{bmatrix} \dot{U}_{c1} \\ \dot{U}_{c2} \\ \dot{I}_{L1} \end{bmatrix} = \begin{bmatrix} 0 & 0 & \frac{u_1}{C_1} \\ 0 & 0 & \frac{u_2}{C_2} \\ -\frac{u_1}{L_1} & -\frac{u_2}{L_1} & \frac{r_1}{L_1} \end{bmatrix} \begin{bmatrix} U_{c1} \\ U_{c2} \\ I_L \end{bmatrix} + \begin{bmatrix} \frac{-I_{dc}}{C_1} \\ \frac{-I_{dc}}{C_2} \\ \frac{U_{pv}}{L} \end{bmatrix} \tag{2}$$

Where I_b, L and I_L are the output current, the storage inductance and the current across it. U_{pv} , U_{C1} and U_{C2} are respectively the PV voltage and the capacitors voltage. u_1 and u_2 are the control signal of the power switches [10].

The voltage across the capacitor 1 and capacitor 2 comprises a resistive and a capacitive term. The equation of the voltage of the two capacitors is given by the following equation:

$$\begin{cases} U_{ca} = U_{c1} + r_1 c_1 . \dot{U}_{c1} \\ U_{cb} = U_{c2} + r_2 c_2 . \dot{U}_{c2} \end{cases} \tag{3}$$

2.2. Wind system modeling

The wind conversion system part comprises blades which convert the wind energy into mechanical power. The blades are directly connected to the synchronous generator PMSG. An AC/DC converter consisting of a three-phase diode rectifier is connected between the wind generator and the common DC bus.

2.2.1. The turbine model

The aerodynamic power P_t captured by the wind turbine is expressed by the following relation [19-20].

$$P_t = \frac{1}{2}\pi.\rho.R^2.Cp(\lambda).v^3 \quad (4)$$

Where the tip speed ratio λ is given by

$$\lambda = \frac{R.\Omega_m}{v} \quad (5)$$

v is the wind speed, ρ is the air density, R is the rotor radius and Cp is the power coefficient. The power coefficient is expressed as function of tip speed ratio λ in place of pitch angle β as

$$C_p = 0.576.\left(\frac{116}{\lambda_i} - 0.4\beta - 5\right).e^{\frac{21}{\lambda_i}} + 0.0068.\lambda \quad (6)$$

$$\frac{1}{\lambda_i} = \frac{1}{\lambda+0.08\beta} - \frac{0.035}{\beta^3+1} \quad (7)$$

The aerodynamic power is also defined by

$$P_t = T_m\,.\,\omega_m \quad (8)$$

Where T_m is the aerodynamic torque and ω_m is the rotor speed. The curve of power in term of the rotor speed and the aerodynamic power in term of the tip speed ratio are illustrated in Figure 5 and Figure 6 respectively.

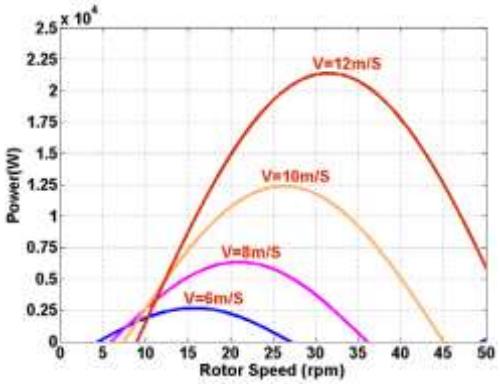

Figure 5. Power curve of the wind generator

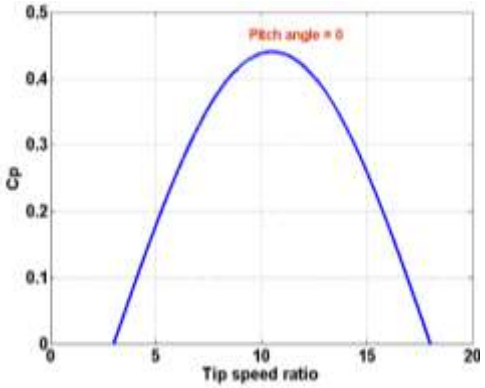

Figure 6. The power coefficient as function of tip speed ratio

In this work, the control of the wind conversion system is carried out keeping the pitch angle equal to zero (β=0). The following mechanical model gives the dynamic of the wind turbine.

$$J\frac{d\omega_m}{dt} = T_m - T_{em} - f.\omega_m \quad (9)$$

Where T_{em} is the electromagnetic torque of the synchronous generator, J is the turbine total inertia and f is the turbine total external damping.

2.2.2. The PMSG model

The dynamic equations of a PMSG generator is written in a synchronously rotating *dq* reference frame as [1].

$$\begin{cases} V_{sd} = -R_s.i_{sd} - L_d \frac{di_{sd}}{dt} + L_q.\omega_r.i_{sq} \\ V_{sq} = -R_s.i_{sq} - L_q \frac{di_{sq}}{dt} - L_d.\omega_r.i_{sd} + \Phi_{st}.\omega_r \end{cases} \quad (10)$$

Where V_{sq} and V_{sd} are the q-axis and d-axis stator voltages. i_{sd} and i_{sq} are the q-axis and d-axis stator currents, R_s is the resistance of the stator windings, $\omega_r = p.\omega_m$ is the linkage produced by the permanent magnet mechanism located in the rotor. The power produced by a PMSG generator is expressed as a function of the dq currents components and the dq voltage components by the following relation.

$$P = \frac{3}{2}.(V_{sd}I_{sd} + V_{sq}I_{sq}) \quad (11)$$

2.2.3. Common DC bus and three-phase inverter model

Figure 7 illustrates the three-phase inverter and the power grid. the three-phase transformer is used to adjust the voltage level. The common DC bus receives the power extracted from the two renewable sources (photovoltaic and wind turbine).

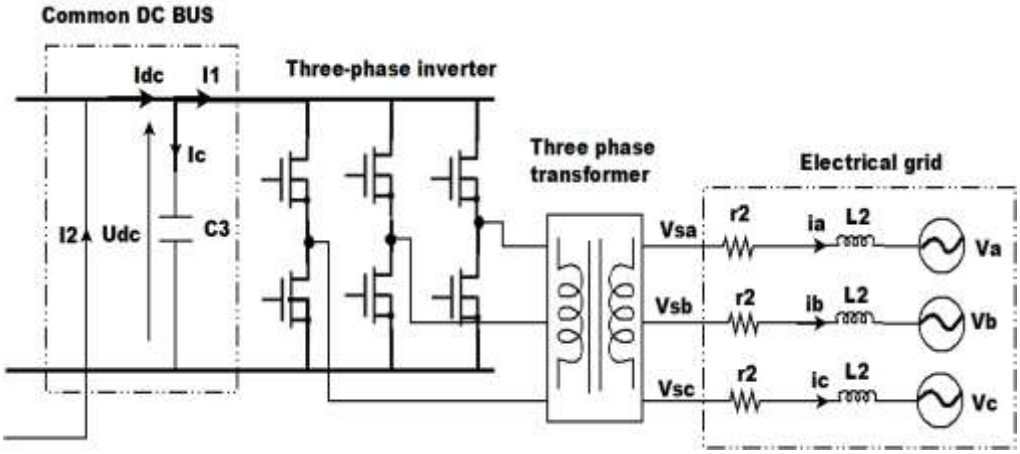

Figure 7. Electrical diagram of the grid side part consisting of a three-phase inverter, transformer and the equivalent model of electrical grid

The equivalent model of the power grid and the three-phase inverter is based on the Park transformation. The equivalent model allows the transfer of maximum power in presence/absence of the energy produced by the photovoltaic/wind source using a single TLBC and an uncontrolled three-phase rectifier. The line voltages are presented in (12) considering L_a=L_b=L_c=L_2 and r_a=r_b=r_c=r_2.

The electrical part of the hybrid system and the electrical grid are described by the following equations.

$$\begin{cases} v_{sa} = r_2 i_a + L_2 \frac{di_a}{dt} + v_a \\ v_{sb} = r_2 i_b + L_2 \frac{di_b}{dt} + v_b \\ v_{sc} = r_2 i_c + L_2 \frac{di_c}{dt} + v_c \end{cases} \quad (12)$$

Where v_{sa}, v_{sb} and v_{sc} are the output voltages of the three-phase transformer respectively. v_a, v_b and v_c are the voltages of the grid side. Applying dq transformation and developing the equations system (12), it is possible to find the differential Equations (13):

$$\begin{cases} L_2 \frac{di_d}{dt} = v_{sd} - \left(r_2 i_d + L_2 \omega_g i_q + v_d\right) \\ L_2 \frac{di_q}{dt} = v_{sq} - \left(r_2 i_q + L_2 \omega_g i_d + v_q\right) \end{cases} \quad (13)$$

Where v_{sd}, v_{sq} are the direct and quadrature components of the output voltage of the three-phase transformer respectively. v_d, v_q are the direct and quadrature components of the grid voltages resepectively. The expression of the active and reactive power injected to the grid are expressed by the following equations:

$$\begin{cases} P_g = v_d i_d + v_q i_q \\ Q_g = v_q i_d - v_d i_q \end{cases} \quad (14)$$

3. DESCRIPTION OF THE CONTROL APPROACH

The control strategy of TLBC is based on the use of two main loops. The extraction of the maximum power of the photovoltaic generator is ensured by a P&O MPPT which provides the reference of the photovoltaic current. The voltage balancing is necessary to have a correct operation of the TLBC. The extraction of the maximum power of the wind generator is ensured by direct access to the DC bus without the use of an additional converter. A sensorless MPPT algorithm provides the DC bus reference voltage which corresponds to maximum power operation of the wind generator. The control of the DC bus voltage constitutes the external control loop of the three-phase inverter. The internal loop consists of a simple PI corrector used for the regulation of the the direct and quadrature currents components injected into the electrical grid. Figure 8 summarizes the control strategy of the TLBC and the three-phase inverter.

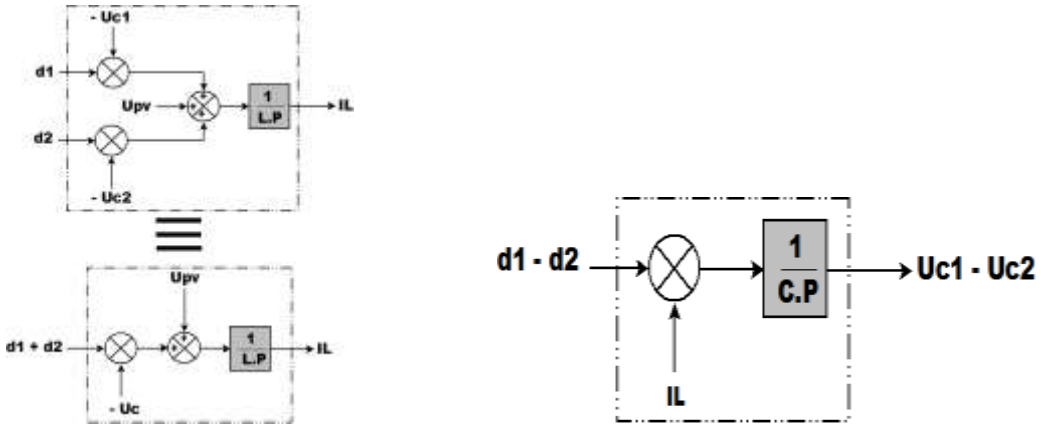

(a) (b)

Figure 8. Average model of the (TLBC), (a) IL as function of d1 + d2 when Uc_1=Uc_2, (b) Uc_1-Uc_2 as function of d_1–d_2

3.1. Control approach of the Three-Level Boost Converter

The TLBC is used to adapt the voltage level of the PV generator to the common DC bus voltage. The TLBC control allows to extract the maximum power of the PV generator by adjusting the PV current to its optimal value. The control loops of the TLBC are constructed according to the following hypothesis:

1. The common DC bus voltage is assumed to be constant. The regulation of the DC bus voltage is ensured by the three-phase inverter control loop.
2. The balancing control loop of the capacitor voltage Uc_1 and Uc_2 is designed to have a faster dynamic than the Ipv current control loop. The adopted control strategy simplifies the synthesis of the Ipv current regulator. The control objectives of the TLBC are summarized in the following points:
   a. balance the capacitor voltages
   b. operate the photovoltaic generator at its maximum power

Using the average equivalent model, the TLBC is described by Figure 8. Where d1 and d2 are are respectively the average value in a cutting period of the control signal u_1 and u_2. The model shown in Figure 8 assumes that the voltage regulation loop of the capacitors Uc_1 and Uc_2 is faster than the current control loop IL. This justifies the hypothesis that the voltages Uc_1 and Uc_2 are balanced in the model given in Figure 8 (Uc_1=Uc_2=U_c). IL, Uc and Udc are considered disturbances which must be compensated during the closed-loop control. The balancing of the capacitor voltages is obtained by regulating the difference Uc_1-Uc_2

to zero and the extraction of the maximum power of the photovoltaic generator is achieved by regulating the current IL to its reference.

Figure 9 illustrates the principle of photovoltaic current regulation and voltage balancing. Disturbance compensation is required to linearise the system. Two proportional-integrally correctors PI are synthesized for PV current regulation and capacitor voltages.

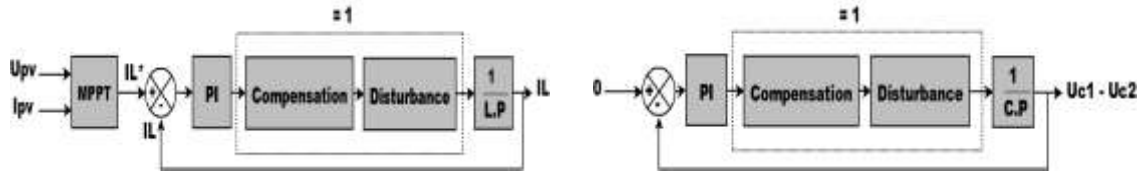

(a) (b)

Figure 9. Closed loop control, (a) IL Current control approach, (b) Balancing voltage control

3.2. DC bus voltage and grid current control approach

The power produced by the PV/wind source is transmitted to the electrical power grid through the three-phase inverter. The control of the inverter allows to regulate the DC bus voltage and to have a quasi-unit power factor.

The reference of the DC bus voltage is obtained by an estimator which provides the optimal value of the DC bus voltage corresponding to maximum power operation of the wind generator. The control of the d-q components of the currents injected into the electrical grid is ensured by considering a decoupling between the adjustment of these two components. The direct component of the current injected into the electrical grid represents the active component that is proportional to the power extracted from the hybrid PV/WIND sources. The quadrature component is dependent on the reactive power and must be regulated to zero. A simple PI regulator is largely sufficient to regulate the d-q components and to obtain a quasi-unit power factor. The principle of voltage oriented control scheme is shown in Figure 10.

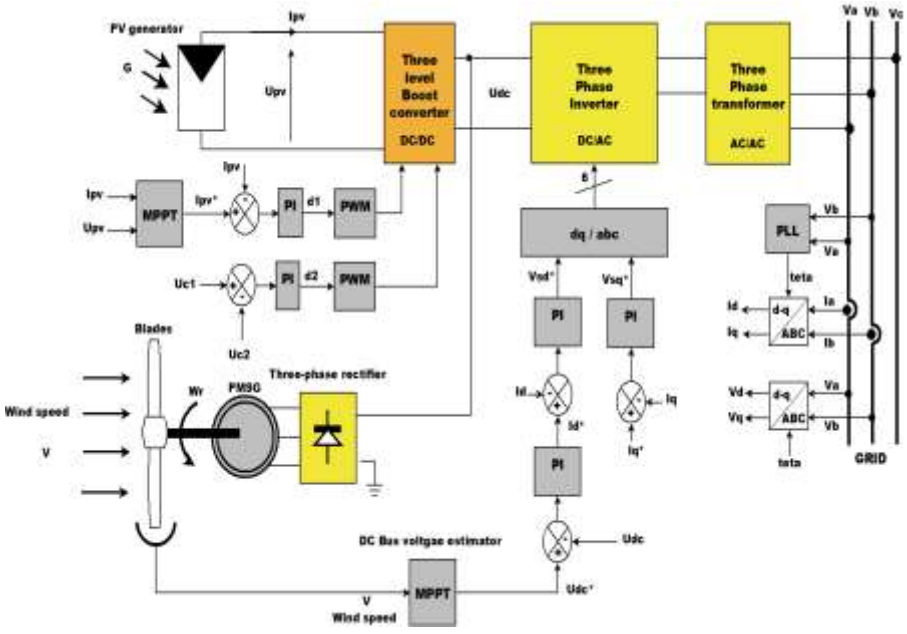

Figure 10. Control strategy of the TLBC and the three- phase inverter

Firstly, the line voltages Vabc are supplied to the PLL which ensures the determination of the angle of the voltages. The calculated angle will be used to d-q coordinate transformation of currents and line

voltages. Then the d-q components of the line currents and the DC bus voltage are used in the design of the decoupled controller. The voltage references calculated by the regulators are modulated by the PWM block (Pulse With Modulation) and the control signals Sabc of the three arms of the inverter are provided (S=1 means upper switch ON, lower switch OFF; S=0 means upper switch OFF, lower switch ON).

In developing Equation (13), it is easy to find the following equation:

$$\begin{cases} v_{sd} = L_2 \frac{di_d}{dt} + r_2 i_d + \left(v_d + L_2 \omega_g i_q\right) \\ v_{sq} = L_2 \frac{di_q}{dt} + r_2 i_q + \left(v_q - L_2 \omega_g i_d\right) \end{cases} \quad (15)$$

The terms $(v_d + L_2 \omega_g i_q)$ and $(v_q - L_2 \omega_g i_d)$ are considered as perturbations which must be compensated.

By applying the Laplace transform to the compensated system, the transfer function of the inverter is given as:

$$\begin{cases} \frac{v_{sd}}{i_d} = \frac{1}{L_2.P + r_2} \\ \frac{v_{sq}}{i_q} = \frac{1}{L_2.P + r_2} \end{cases} \quad (16)$$

A simple (PI) corrector is sufficient to regulate the d-q components i_d and i_q to their references. If the inverter is ideal and has no power losses, the three-phase inverter is equivalent to a gain G equal to 1.

The references of the I_d and I_q components are respectively provided by the control loop of the DC bus voltage and the reactive power. Considering the orientation of the dq voltages (v_q=0), the equations (14) becomes:

$$\begin{cases} P_g = v_d i_d \\ Q_g = -v_d i_q \end{cases} \quad (17)$$

From these relations, it is possible to impose the active and reactive power reference, denoted by Pg* and Qg *, imposing reference currents I_d* and I_q*:

$$\begin{cases} I_d * = \frac{P_g *}{V_d} \\ I_q * = \frac{Q_g *}{V_d} \end{cases} \quad (18)$$

The direct current component is used to control the active power at the connection point of the hybrid system to the grid. The quadrature component is used to regulate the reactive power. Figure 11 summarizes the regulation principle of the d-q components of line currents.

To determine the angles required for Park transformations for line currents and voltages, a PLL (Phase Locked Loop), as illustrated in Figure 12, is used. The PLL accurately estimate the frequency and amplitude of the mains voltage.

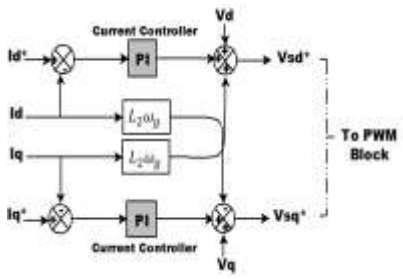

Figure 11. Decoupled controller of the d-q components of line currents

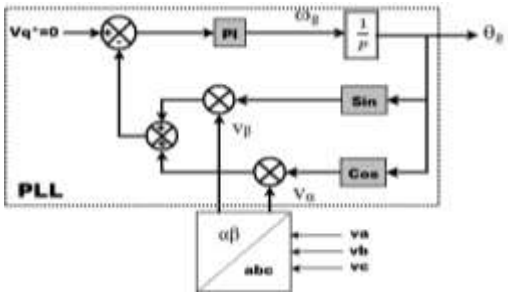

Figure 12. Establishment of transformation angles using PLL

The dynamics of the voltage across the DC bus capacitor is given by the following relation:

$$I_{c3} = \frac{dU_{dc}}{dt} = I_{dc} - I_1 \quad (19)$$

According to Figure 7, the power exchange between the DC bus at the input of the three-phase inverter is described by the following relation:

$$\begin{cases} P_{dc} = V_{dc}.I_{dc} \\ P_c = V_{dc}.I_{c3} \\ P_{ond} = V_{dc}.I_1 \end{cases} \quad (20)$$

The equality of the sum of the powers produced by the PV/Wind sources and the power transmitted to grid at the input of the three-phase inverter is described by the relation (21):

$$P_{dc} = P_c + P_{ond} \quad (21)$$

If the losses in the inverter are neglected, the power transmitted to the grid is equal to the power produced:

$$P_g = P_{dc} = P_c + P_{ond} \quad (22)$$

By regulating the power transmitted to the grid, it is possible to control the power P_c in the capacitor and thus to regulate the DC bus voltage. To determine the power reference Pg*, the powers P_{ond} and P_c must be known. The reference power of the DC bus capacitor is connected to the current reference flowing in the capacitor:

$$P_c * = V_{dc}.I_c * \quad (23)$$

Figure 13 shows the block diagram of the DC bus voltage control. To simplify the synthesis of the (PI) regulator, the internal current loop is assumed to be unitary (Id=Id*) since the internal loop is assumed to be faster than the external loop.

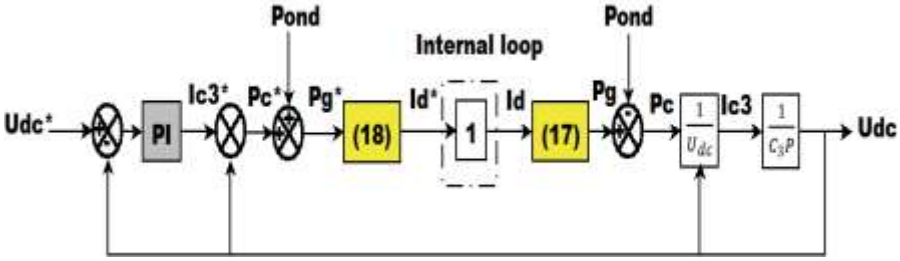

Figure 13. Block diagram of the dc bus voltage control

4. SIMULATION RESULTS

The model of the PV, Wind generators, the MPPT algorithms, the control of the DC/DC converter and the DC/AC inverter are implemented in Matlab/Simulink. In this study, the PV/wind generators deliver a maximum power of 10 kwatts and 22 kwatts respectively. The specification of the control parameters and the main characteristics of the hybrid system are summarized in Table 1, Table 2 and Table 3.

Table 1. Parameters Used in the Simulation

	Parameters	Value	Unit
Three	L_1	2	mH
Level	C1	470	µF
Boost	C2	470	µF
Converter	f	20 k	Hz
MPPT	Step	0.001	-

Table 2. Main Characteristics of the PV Generator

	Parameters	Value	Unit
PV Generator	P_{max}	10.2	kW
	U at P_{max}	220	V
	U_{oc}	260	V
	I_{cc}	46	A

Table 3. Main Characteristics of the Wind Turbine and PMSG

	Parameters	Value	Unit
Turbine	Vt_n	12	m/s
	R (radius)	4	m
PMSG	U_s	500	V
	P_n	22	kW
	f	50	Hz
	R_s	50 m	Ω
	$L_d = L_q$	0.6 m	H
	J_m	0.011	$kg.m^2$
	P	10	-

During the simulation stage, the hybrid system is subjected to sudden changes in wind speed and solar irradiation. The irradiation and wind speed profiles are illustrated in Figure 13(a) and Figure 14(a).

Figure 14(b) shows the PV current and its reference. According to Figure 14(b), it is found that the PV current follows its reference. In transient mode, the PV current reaches its reference after 1.2 seconds. During an abrupt change in irradiation (at time t=7S), the PV current took about 0.3S to reach its reference. It is noted at times t=3S and at time t=5S, the PV current deviates from its reference value because it is influenced by a wind speed change which has created a momentary imbalance in the power injected into the grid. It is understandable that the control acts quickly to guaranty the equilibrium and stability of the PV current.

Figure 14(c) shows the PV power in response to the irradiation step. The power follows the maximum value according to the available irradiation. According to power curve given in Figure 3(b), the irradiation of $800W/m^2$ and $1000W/m^2$ corresponds approximately to 8250W and 10350W respectively. Depending on the irradiation levels, Figure 14(c) shows that the PV generator operates at its maximum power since the average operating power is equal to 8230W and 10340W respectively. The efficiency of the (MPPT) algorithm is calculated by the following relation:

- G=800W/m^2 the efficiency is $\eta_{G1} = \frac{P_{pv}}{P_{\max\_curv}} = \frac{8230}{8250} = 99{,}75\ \%$
- G=1000W/m^2 the efficiency is $\eta_{G2} = \frac{P_{pv}}{P_{\max\_curv}} = \frac{10340}{10350} = 99{,}9\ \%$

According to Figure 14(d), the capacitor voltages Uc_a and Uc_b are well balanced. The changes in wind speed at times t=3S and t=5S and the change in solar irradiation at time t=7S did not influence the balancing of the capacitor voltages. The transient regime took a few milliseconds before the control loop adjusts the voltages to half of the DC bus voltage. The dynamics of the capacitor voltages shows that the hypothesis reported during the synthesis of the PI current regulator is correctly verified. According Figure 14(d), the proposed control maintain these voltages well balanced.

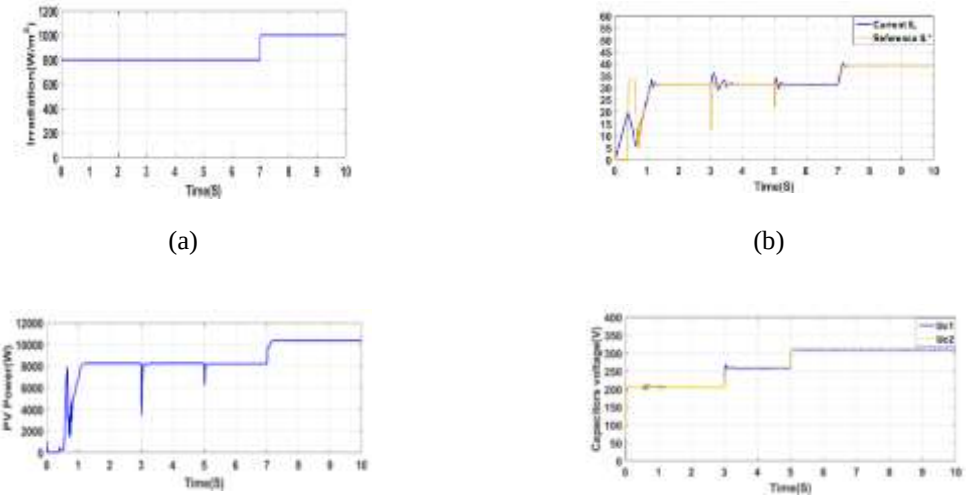

(a) (b)

(c) (d)

Figure 14. (a) Irradiation step (W/m^2, (b) Inductor current (A), (c) PV power (W), (d) Capacitor voltages(V)

In the following simulations, the wind blades are subjected to a wind speed profile according to Figure 15(a).

The reference of the DC bus voltage is estimated as a polynomial function of the wind speed. Figure 15(b) shows the DC bus voltage and its reference. It noted that the DC bus voltage follows its reference.

Figure 15(c) illustrates the wind power. According to power curve given in Figure 5, the theoretical values of the maximum powers of 8m/S, 10m/S and 12m/S are 6350W, 12500W and 21250W respectively.

Figure 15(c) shows that the average powers of the previously indicated wind speeds are 6280W, 12250W and 21100W respectively. It noted that the simulation and the theoricals results are similar. The numerical values of the efficiency are calculated:

- v=8m/S the efficiency is $\eta_{v1} = \frac{P_{wind}}{P_{\max\_curv}} = \frac{6280}{6350} = 98,89\ \%$
- v=10m/S the efficiency is $\eta_{v2} = \frac{P_{wind}}{P_{\max\_curv}} = \frac{12250}{12500} = 98\ \%$
- v=12m/S the efficiency is $\eta_{v2} = \frac{P_{wind}}{P_{\max\_curv}} = \frac{21100}{21250} = 99{,}29\ \%$

Figure 15(d) shows the power coefficient. According to Figure 6, the optimal value of the power coefficient is 0.45. The Figure 15(d) shows that the power factor is well maintained at its optimal value, which proves that the wind generator operates at a maximum power. The power coefficient deviates from its optimal value at times t=3S and t=5S due to the changes in the wind speed. The control system adjusts the power coefficient to its optimal value within the shortest time.

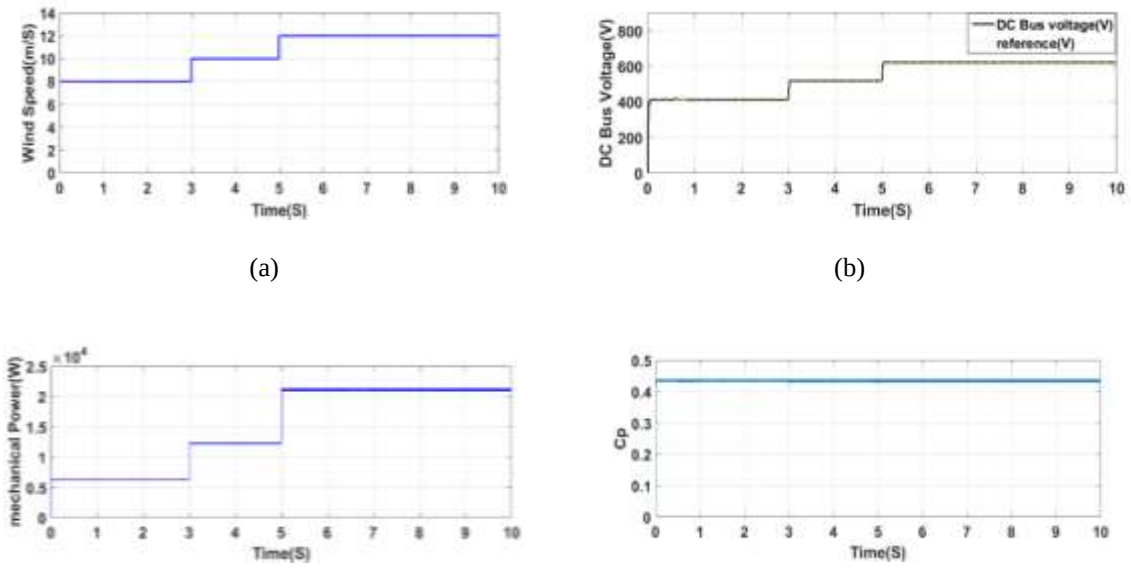

(a) (b)

(c) (d)

Figure 15. (a) Wind speed (m/S), (b) DC bus voltage (V), (c) Wind power (W), (d) Power cefficient

Figure 16(a) illustrates the current injected into the grid. The increase in the power provided by the PV and wind generators implies an increase in the power injected into the grid. The result is an increase of the Root-Mean-Square (RMS) current since the RMS voltage is imposed by the grid.

Figure 16(b) shows the current and the grid voltage. According to Figure 16(b), the current and voltage are in phase. It can be deduced that the power factor at the connection between the hybrid system and the grid is quasi-unitary and the reactive power injected into the grid is zero.

Figure 16(c) illustrates the spectrum of the current injected into the grid. It is observed that the spectrum comprises the fundamental component of 50Hz frequency, the amplitude of which is the largest and the components of odd frequencies of the fundamental (3, 5, 7 and 9). The signal distortion rate is equal to 7.07%.

Figure 16(d) shows the overall efficiency of the hybrid system. It noted that the average value of the efficiency is equal to 90% under the various climatic conditions. It observed that there is a decrease in the efficiency at times t=3S and t=5S and t=7S and then quickly returns to its value. 10% of the power extracted from the PV/Wind generators is lost in the power conversion structure. The power losses are due to the Joule effect, the (MPPT) method and the switching losses of the power switches.

The Figure 17 illustrates the spectrum of injected currents in the case of a hybrid PV/Wind system based on two DC/DC converters.

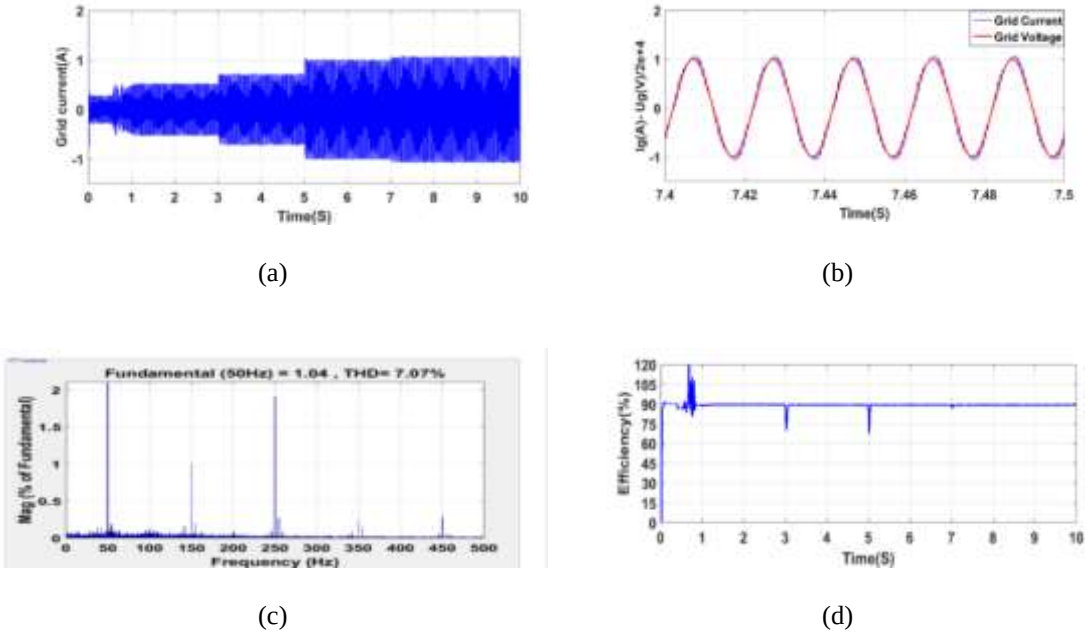

Figure 16. (a) Grid current (A), (b) Grid current (A) and voltage (V), (c) Spectrum of the grid current, (d) Hybrid PV/WIND efficiency (%)

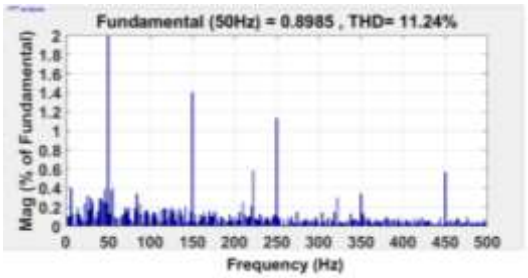

Figure 17. Spectrum of injected currents in the case of a hybrid PV/Wind system based on two DC/DC converters

The following table shows the rate of harmonics injected into the power grid. The table below compares the distortion ratio and the percentage of harmonics (order 3, 5, 7 and 9) produced in the case of a hybrid PV/wind system based on two DC/DC converters and in the case of proposed system based on a single DC/DC converter.

Except for the harmonic of order 5, it is remarkable that the rate of harmonics injected using the proposed hybrid system is lower than the harmonic rate of a hybrid system based on two DC/DC converters. In addition, the ratio of distortion of injected currents is lower (7.07% instead of 11.24%). According to the simulations results, the quality of the electrical energy produced using the proposed structure is better compared to the quality of the energy produced by a hybrid system based on two DC/DC converters.

Table 4. Injected Current Harmonics (Normalized to Fundamental) and its THD Value

Harmonic order (n)	(In/I1) % Hybride PV/Wind sysem Based 2 DC/DC Converters	(In/I1) % Hybride PV/Wind sysem Based single DC/DC Converter
3	1.4 %	1%
5	1.1%	1.8%
7	0.35%	0.25%
9	0.55%	0.55%
THD	11.24%	7.07%

5. CONCLUSION

This paper deals with the study of modeling and control of a hybrid PV/Wind sources. The proposed structure consists of a single DC/DC converter and a DC/AC inverter. In this study, the operating principle of the hybrid system is well explained and the elements constituting the proposed power conversion structure are modeled. The dynamic model of DC/DC is developed considering the imperfections of the passive components. To synthesize the correctors, a linearization is proposed since the (TLBC) exhibits a nonlinear behavior. Using disturbance compensation, the transfer function of the (TLBC) is approximated by a first order system and a simple (PI) corrector is used to regulate the PV current and to balance the capacitors voltages. The wind generator is connected directly to the DC bus through the uncontrolled three-phase rectifier. Maximum power operation is achieved by controlling the common DC bus voltage. The reference of the bus voltage is estimated by a polynomial function of the wind speed. To ensure a transfer of the extracted PV/Wind power with a power factor close to unity, a control approach based on the principle of vector control is used. Decoupling between the state variables is necessary which allowed to linearise the transfer function of the three-phase inverter. Using the principle of the disturbance compensation, a (PI) correctors are synthetised to regulate the DC bus voltage and the direct and quadrature components of the injected currents. The simulation results prove that the proposed hybrid conversion structure has better performance in terms of maximum power extraction and injection into the power grid. The use of two complementary sources has allowed a good reliability under varying climatic conditions.

The simulations results show that the control approaches based on the linearisation of static converters and the use of a variable DC bus voltage for the extraction of the maximum power of the wind generator are well validated. The proposed structure based on a single DC/DC converter looks promising since it has several advantages in comparison with the conventional structure based two DC/DC converters. The use of a single DC/DC converter allows a better quality of the electrical energy injected into the grid because there is a limitation of the amplitude of the harmonics produced and a better distortion ratio. In addition, the limited joules losses (better overall efficiency of the structure) and the reasonable cost of the proposed PV/Wind system are sufficient reasons for choosing this structure. One of the applications of the proposed structure is to be integrated as a base unit of a PV/wind farm that produces electrical energy at medium voltage, to meet local energy needs and to inject the surplus to the distribution grid.

REFERENCES

[1] M. H. Nehrir, B. J. Lameres, G. Venkataramanan, V. Gerez and L. A. Alvarado, "An approach to evaluate the general performance of stand-alone wind/photovoltaic generating systems," in *IEEE Transactions on Energy Conversion*, vol. 15, no. 4, pp. 433-439, Dec. 2000.

[2] J. Tian, Z. Liu, J. Shu, J. Liu and J. Tang, "Base on the ultra-short term power prediction and feed-forward control of energy management for microgrid system applied in industrial park," in *IET Generation, Transmission & Distribution*, vol. 10, no. 9, pp. 2259-2266, 9 6 2016.

[3] Li Wang and T. Lin, "Stability and Performance of an Autonomous Hybrid Wind-PV-Battery System," *2007 International Conference on Intelligent Systems Applications to Power Systems*, Toki Messe, Niigata, 2007, pp. 1-6.

[4] F. Valenciaga and P. F. Puleston, "Supervisor control for a stand-alone hybrid generation system using wind and photovoltaic energy," in *IEEE Transactions on Energy Conversion*, vol. 20, no. 2, pp. 398-405, June 2005.

[5] Hung-Cheng Chen, Jian-Cong Qiu and Chia-Hao Liu, "Dynamic modeling and simulation of renewable energy based hybrid power systems," 2008 Third International Conference on Electric Utility Deregulation and Restructuring *and Power Technologies*, Nanjing, 2008, pp. 2803-2809.

[6] F. Giraud and Z. M. Salameh, "Steady-state performance of a grid-connected rooftop hybrid wind-photovoltaic power system with battery storage," in *IEEE Transactions on Energy Conversion*, vol. 16, no. 1, pp. 1-7, March 2001.

[7] H. C. Chiang, T. T. Ma, Y. H. Cheng, J. M. Chang and W. N. Chang, "Design and implementation of a hybrid regenerative power system combining grid-tie and uninterruptible power supply functions," in *IET Renewable Power Generation*, vol. 4, no. 1, pp. 85-99, January 2010.

[8] S. Bae and A. Kwasinski, "Dynamic Modeling and Operation Strategy for a Microgrid With Wind and Photovoltaic Resources," in *IEEE Transactions on Smart Grid*, vol. 3, no. 4, pp. 1867-1876, Dec. 2012.
[9] K. Hu and C. Liaw, "Incorporated Operation Control of DC Microgrid and Electric Vehicle," in *IEEE Transactions on Industrial Electronics*, vol. 63, no. 1, pp. 202-215, Jan. 2016.
[10] Daniel, S.A., Pandiraj, K., Jenkins, N., "*Control of an integrated wind turbine generator and photovoltaic system for battery charging*," Proc. British Wind Energy Conf, 1997, 121–128.
[11] M. M. R. Singaravel and S. A. Daniel, "MPPT With Single DC–DC Converter and Inverter for Grid-Connected Hybrid Wind-Driven PMSG–PV System," in *IEEE Transactions on Industrial Electronics*, vol. 62, no. 8, pp. 4849-4857, Aug. 2015.
[12] B. Yin, R. Oruganti, S. K. Panda and A. K. S. Bhat, "A Simple Single-Input–Single-Output (SISO) Model for a Three-Phase PWM Rectifier," in *IEEE Transactions on Power Electronics*, vol. 24, no. 3, pp. 620-631, March 2009.
[13] A. V. Stankovic and K. Chen, "A New Control Method for Input–Output Harmonic Elimination of the PWM Boost-Type Rectifier Under Extreme Unbalanced Operating Conditions," in *IEEE Transactions on Industrial Electronics*, vol. 56, no. 7, pp. 2420-2430, July 2009.
[14] P. Shanthi, G. Uma and M. S. Keerthana, "Effective power transfer scheme for a grid connected hybrid wind/photovoltaic system," in *IET Renewable Power Generation*, vol. 11, no. 7, pp. 1005-1017, 7 6 2017.
[15] Sameh Zenned, Emna Aridhi, Abdelkader Mami, "Modeling, Control of Micro-grid Powered by Solar and Wind Energies," *International Journal of Power Electronics and Drive System (IJPEDS)*, vol. 8, no. 1, 2017, 402-416
[16] Hassan Abouobaida, EL Beid Said, "Practical Performance Evaluation of Maximum Power Point Tracking Algorithms in a Photovoltaic System," *International Journal of Power Electronics and Drive Systems*, vol 8, no 4, 2017, pp. 1744-1755
[17] A. Naderipour, A. Asuhaimi Mohd Zin, M. H. Habibuddin, M. Mortadi, M. Miveh, H. N. Afrouzi, "A New Compensation Control Strategy for Grid-connected Wind Turbine and Fuel Cell Inverters in a Microgrid," *International Journal of Power Electronics and Drive System*, vol. 8, no. 1, 2017, 272-278
[18] Hassan Abouobaida, Said El Bied, "New Optimization Method of the MPPT Algorithm and Balancing Voltage Control of the Three-Level Boost Converter (TLBC)," *International Journal of Applied Power Engineering*, vol.6, no.2, 2017, pp. 114-123
[19] Sarita Samal, Prakash Kumar Hota, "Power Quality Improvement by Solar Photo-voltaic/Wind Energy Integrated System Using Unified Power Quality Conditioner," *International Journal of Power Electronics and Drive System*, vol. 8, no. 3, 201 7, 1416-1426
[20] H. Abouobaida and E. Beid Said, "New MPPT control for wind conversion system based PMSG and a comparaison to conventionals approachs," *2017 14th International Multi-Conference on Systems, Signals & Devices (SSD)*, Marrakech, 2017, pp. 38-43.